Drivers of Forest Structural Complexity in Mountain Forests of Nepal

Authors: Basnet, Prakash, Das, Smita, Hölscher, Dirk, Pierick, Kerstin, and Seidel, Dominik

Drivers of Forest Structural Complexity in Mountain Forests of Nepal

Prakash Basnet[1]*, **Smita Das**[2], **Dirk Hölscher**[2], **Kerstin Pierick**[1], and **Dominik Seidel**[1]

* Corresponding author: pbasnet@uni-goettingen.de

[1] Department for Spatial Structures and Digitization of Forests, University of Göttingen, Büsgenweg 1, 37077 Göttingen, Germany
[2] Tropical Silviculture and Forest Ecology, University of Göttingen, Büsgenweg 1, 37077 Göttingen, Germany

Forests in the Himalayan region are crucial for maintaining the region's ecological balance, conserving biodiversity, and supporting the livelihoods of local people. However, because of limited accessibility and an adverse climate, scientific studies on how forest functions in this region depend on ecological drivers are rare. We used a handheld mobile laser scanner to assess the forest structural complexity (FSC) in the Annapurna Conservation Area of Nepal and related this to its potential drivers, including forest disturbances. Based on stratified sampling, we selected 69 plots across a gradient of elevations and precipitations. Other factors that might influence FSC were obtained from forest inventory data, climatic databases, the Google Earth platform, and digital elevation models. Using simple linear regression and multiple regression analysis, we tested for the dependency of FSC, measured using the box dimension (D_b), on influential predictor variables. Overall, explanatory variables strongly influenced FSC (adjusted $R^2 = 0.60$, $P < 0.001$), with D_b being affected by the number of trees, the maximum height of the forests, species diversity, north-facing aspect, soil pH, and forest disturbance. Surprisingly, climatic variables, precipitation, and temperature did not show any effect on FSC. The LiDAR-based approach to FSC used in our study enabled rapid assessment in hard-to-access regions. It can be used to inform effective management and conservation, for example, in monitoring development over time or for benchmarking.

Keywords: Himalayan forests; LiDAR; handheld mobile laser scanning; box dimension; tree architecture.

Introduction

Mountain landscapes are unique and diverse, boasting remarkable natural and cultural diversity. Mountain regions sustain a quarter of the world's terrestrial biodiversity (Rahbek et al 2019). The highest mountains on Earth are found in the Himalayas (Miehe et al 2015), an underexplored and particularly vulnerable geographical area. This results from the harsh weather conditions, treacherous terrain, limited accessibility, climate change, and habitat degradation (Schmeller et al 2022).

The forests in this region play a crucial role in maintaining ecological, economic, and sociocultural stability (Dasgupta and Shakya 2023). Many local inhabitants rely heavily on forests for their livelihoods and for environmental benefits. Unfortunately, climate change and its associated risks, such as glacial lake outburst floods, land degradation, deforestation, and uncontrolled wildfires, are threatening the forests in this area (Wiltshire 2014; Chaudhary et al 2016; Wang et al 2019). This, in turn, affects their productivity, the biodiversity they host, and other ecosystem functions they provide (Kattel 2022). Therefore, it is crucial to obtain evidence-based knowledge on the driving forces for the development of these forests (Shahgedanova et al 2021). In this context, studying forest structure and its drivers is particularly helpful in understanding ecosystem functioning and managing forests accordingly. These drivers can be useful in developing a holistic approach to managing socioecological systems, assessing the vulnerability of climate change impacts, and implementing adaptation strategies through sustainable resource management and biodiversity conservation (Ehbrecht et al 2021; Verma et al 2021).

Forest structural complexity (FSC) is relatively straightforward to measure. It relates to forest carrying capacity (Walter et al 2021), habitat quality (Braunisch et al 2019), productivity (Ma et al 2022), adaptative capacity and resilience (Seidel and Ammer 2023), and forest vitality (Heidenreich and Seidel 2022). Therefore, information on FSC, as a proxy for these ecosystem functions and services, can be useful in making management and conservation decisions, especially in largely understudied systems like Himalayan forests.

The objective and holistic measurement of FSC, defined as all-dimensional, architectural, and distributional patterns of plant individuals and their organs in a given space at a given time (Seidel et al 2020), is possible using LiDAR (light detection and ranging) technology, known as laser scanning. It has proved particularly useful in capturing forest structures comprehensively, efficiently, and in great detail (Ehbrecht et al 2017; Atkins et al 2018; Stiers et al 2018; Heidenreich and Seidel 2022; Neudam et al 2022).

To understand the factors that determine FSC, earlier studies investigated the effects of management (eg Seidel et al 2016; Stiers et al 2018; Asbeck and Frey 2021; Willim et al 2022), anthropogenic activities (Verma et al 2021), seasonality (Neudam et al 2022), diversity (Juchheim et al 2019), climate (Ehbrecht et al 2017), tree attributes (Barbeito et al 2017; Atkins et al 2018; Qi et al 2022), and edaphic properties (Ali et al 2019). Other research has explored the relationship between FSC and climatic conditions on a global scale (Ehbrecht et al 2021). However, there is a lack of understanding regarding these patterns in mountainous areas. Further studies are needed to understand the influence of these and other potentially important factors on FSC in mountain ecosystems.

Our study focused on determining the drivers contributing to FSC in the Himalayan region. We hypothesized that FSC in this region is naturally largely reliant on forest factors, such as the forest type (eg coniferous or deciduous), and on additional environmental factors, such as climatic and topographical factors and human disturbances.

Material and methods

Study area

We conducted research in the Annapurna Conservation Area (ACA), which is located between 28°13′59″N to 29°19′52″N and 83°28′45″E to 84°28′04″E. It is Nepal's largest protected area, spanning 7629 km^2, and includes the Annapurna Himalayan range, with the highest peak reaching 8091 masl. The southern region of the Himalayas in this area is windward, resulting in high precipitation, whereas the northern part is on the leeward side and has lower precipitation. As a result of this natural gradient, most forests are situated in the southern part, with only few forests in the northern foothills range.

A stratified sampling approach was chosen to cover dominant forest types across precipitation and elevational gradients, ensuring spatial coverage of the major forests of the area. This was done by dividing the whole study area into the leeward side and windward side of the Annapurna Himal. We consulted the ACA project office and reviewed Nepal's forest resource assessment report to identify the ACA forest types. The fieldwork was conducted by 2 researchers and ACA project field staff between September and December 2021. The design used was originally developed to validate biomass data from the Global Ecosystem Dynamics Investigation (GEDI), a spaceborne LiDAR mission that creates detailed 3D maps of forests to measure their structure and biomass worldwide (Dubayah et al 2022). We used 69 circular plots with a diameter of 25 m (Figure 1), which were based on GEDI's footprint coordinates taken at least 300 m apart from each plot.

Laser scanning

We used a handheld mobile laser scanner (HMLS; ZEB-Horizon/GeoSLAM Ltd, Nottingham, United Kingdom) to obtain detailed 3D maps of the forest plots. This device, equipped with 16 time-of-flight laser sensors, captured the surrounding area in 3D within a distance of 100 m while being carried through the forest. The scanner's laser wavelength is 903 nm, and it captures up to 300,000 points per second (GeoSLAM Ltd). We started scanning from the plots' centers and moved toward their boundary, and then we continued scanning around the boundary line before crisscrossing the area and ending back at the center. The number and extent of the crisscrossing walks depended on the overall density of the vegetation on the plots, with dense plots requiring more crisscrosses for full capture. Although it is difficult to estimate the degree of completeness and the overall homogeneity of a point cloud from HMLS, there is some evidence that the procedure produces point clouds that are sufficiently dense and comprehensive to reliably calculate FSC (Neudam et al 2022; Mathes et al 2023).

Point cloud processing

Raw data were converted into text format files, along with each trajectory file (scanning path line) using GeoSLAM Hub version 6.1 software (GeoSLAM Ltd). Then, the text files were imported into LiDAR360 version 5.0 software (GreenValley International, California, USA) for postprocessing. We used the software's forestry module to remove outliers in the point cloud data caused by either high-flying objects, such as birds, or low-level error, such as the multipath effect of a laser pulse during scanning. After this, a ground normalization process was conducted using the point cloud's elevation data (z value) to remove the topographical relief effect on the point cloud. To do this, point clouds must be classified into ground and nonground points. We organized ground point classification based on the software's plot terrain and parameter default values. Plots were subjectively assigned into 4 categories according to terrain conditions—flat, gentle, steep, and hilly—to improve the final normalization via the ground points.

To ensure smooth and uniform point clouds, we applied a point subsampling technique with minimum spacing of 0.01 m and a noise filter with a 0.1-m radius. Despite scanning a 25-m plot diameter on the ground, most plots featured sloped terrain (up to 42° inclination measured using an Abney level), necessitating the use of a slope-adjusted area. To account for this, we applied a slope correction factor using the plot radius multiplied by the cosine of the slope angle (Kleinn et al 2002). Next, we clipped the point clouds based on the corresponding adjusted diameter (horizontal distance) for each plot. The clipped point clouds were then converted into xyz files and exported for computing plot-level FSC. Finally, we calculated the box dimension (D_b) as a measure of FSC using Mathematica software (Wolfram Research, Champaign, IL, USA), as described in Seidel (2018); Seidel, Ehbrecht, Annighöfer, et al (2019); and Neudam et al (2022). We chose to use D_b because it is a holistic measure of FSC (Mandelbrot 1982) that considers all elements in a scanned scene and integrates them into a single number (the D_b value), thereby using the full potential of the laser technology. In short, to determine D_b, the forest point cloud is virtually enclosed in boxes of different sizes and the change in the number of boxes needed to enclose all points and the size of these boxes are contrasted. D_b is then defined as the slope of the regression line between the logarithm of the number of boxes on the y axis and the logarithm of the size of the box (relative to the initial size) on the x axis (inverted x axis). We began with the largest box equal to the minimum bounding box of the scanned plot and stopped at the smallest box size,

FIGURE 1 Study area with the boundary of ACA and forest area (shaded area; Potapov et al 2021), including the research plots (black circles). The blank nonforest region consists of bare rock, snow, glaciers, rangelands, and landscapes without vegetation. The dashed lines on the map indicate contour lines in metric units and meters above sea level.
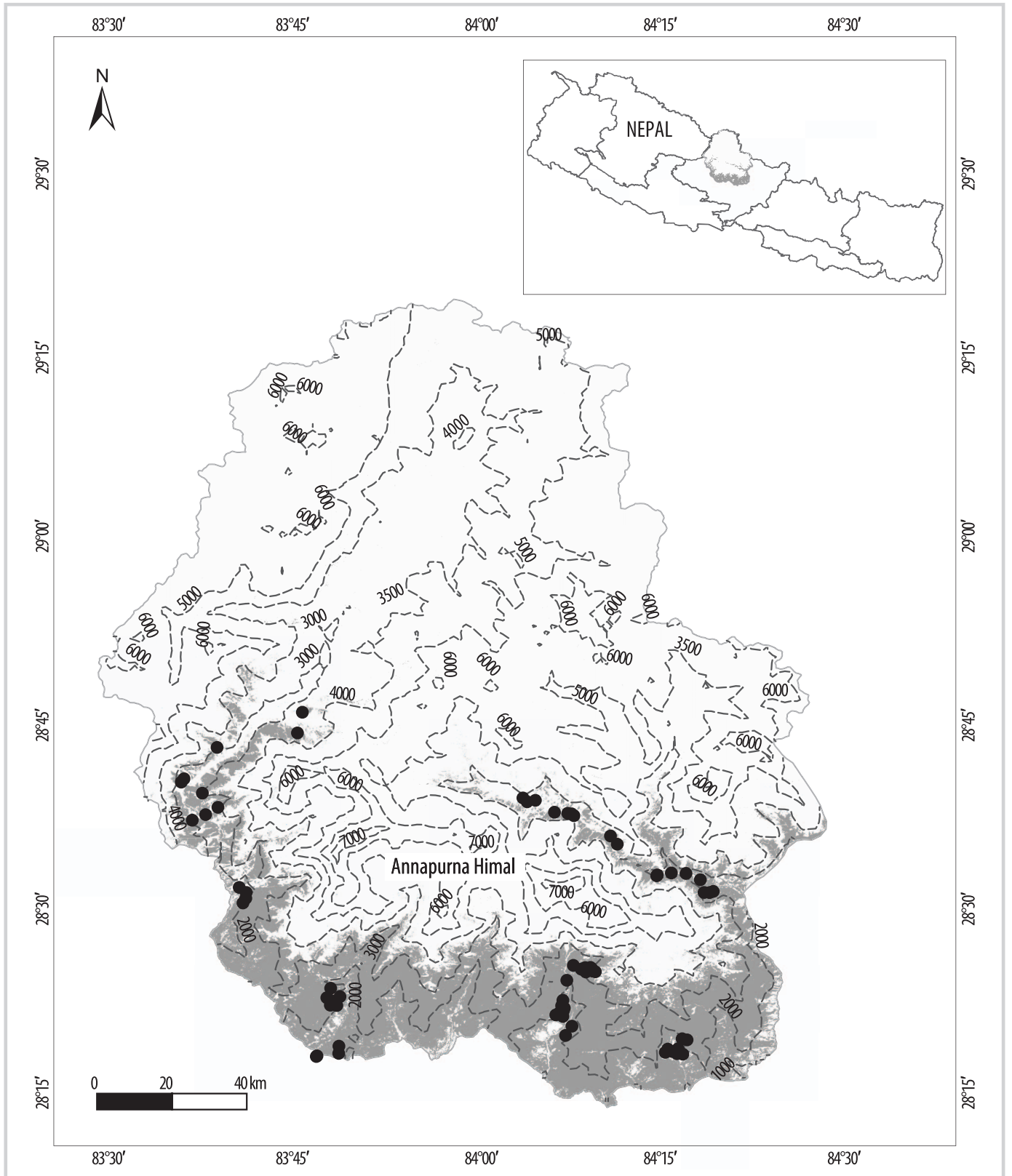
which was never smaller than $20 \times 20 \times 20$ cm, ensuring that we did not sample empty space between laser points because of occlusion. This is conservative but proved to be sufficient in earlier studies to discover spatial differences on small scales (eg Neudam et al 2022) while largely compensating for the occlusion effect (Mathes et al 2023).

Explanatory variables

Forest factors: In each plot, we counted all tree stems with a diameter greater than 10 cm and identified their respective species. When we had difficulty identifying certain species, we took pictures of their leaves, flowers, and fruits and sought the assistance of a botanist to ensure accurate forest species identification. We classified all plots into 3 distinct plant functional types: evergreen broadleaf tree (EBT), deciduous broadleaf tree (DBT), and evergreen needleleaf tree (ENT). This was done based on the dominant species from visual assessment. The maximum height (MH) of the forests at the 98th percentile (meaning 98% of all laser hits were recorded below this height) was calculated from the point clouds (z values) using an algorithm written in Mathematica software.

Soil and topographical factors: We used a Garmin GPSMap 62s device (Garmin Ltd, USA) to measure the plot center's elevation above sea level. To determine the topographical aspect of the plots, we relied on an available digital elevation model (NASA JPL 2013). The slope of the plot's ground was measured using an Abney level (Sokkia No. 8047-4, Japan) from the bottom to the upslope side. The average soil pH value was obtained from SoilGrid maps, which use a 250-m spatial grid and include data from 6 soil profiles at varying depths between 0 and 200 cm (Poggio et al 2021). We were aware that these data might be coarse in spatial resolution but considered them beneficial to test for their explanatory power.

Climatic factors: We obtained climate data from the CHELSA version 2.1 database at a grid-cell resolution of 0.0083° from 1981 to 2010 (Karger et al 2017). The data include accumulated annual precipitation (in millimeters per year) and mean annual temperature (MAT) of the air (in degrees Celsius).

Disturbance factors: During fieldwork, we identified both human-induced and natural disturbances in plots. These included timber and firewood harvesting, land use change, forest fires, cattle grazing, landslides, and flooding during the monsoon season. Because it was not possible to fully reconstruct the land use and disturbance history of the plots, we had to coarsely classify disturbance levels in the field based on visible criteria, such as the extent of firewood and timber collection, livestock grazing, and evidence of forest fire. We categorized each plot as either undisturbed, moderately disturbed, or highly disturbed. In addition, we used Google satellite imagery (Google Earth Pro 7.3.6.9345, 64 bits) and QGIS (version 3.22.7-Biaowieża) to locate the plot and nearby human settlements. Here, a human settlement was considered a house or residential infrastructure (gardens, etc, but not roads) as visually identified in the imagery. We measured the shortest distance along pathways and roads to obtain a more quantitative measure of disturbance likelihood. We assumed

forests located near human settlements within accessible distance were more likely to be affected by human activities.

Statistical analysis

All statistical analyses were conducted in the R programming software (R Core Team 2023). We used 2 statistical approaches to determine which factors affect FSC (D_b) at the plot level, to separate models for all explaining variables, and for multiple regression.

First, we conducted simple linear regressions for continuous predictors and Kruskal–Wallis rank sum tests for categorical predictors, followed by Dunn tests for post hoc analysis. This helped us identify general patterns of D_b across gradients and forest categories. Data inspection showed a clear hump-shaped pattern for the relationship of D_b with MH. Therefore, in this case, a 3-degree polynomial regression model was fitted. Nonparametric Kruskal–Wallis and Dunn tests were conducted to compare differences of D_b between levels of categorical predictors in the *ggpubr* (version 0.6.0) and *ggplot2* (version 3.4.3) packages in R (Kassambara 2023).

Second, we used multiple linear regression with a model selection process to find a combination of predictor variables that explained FSC well. Before fitting the multiple linear regression, we assessed the Pearson correlation coefficient r of all pairs of continuous variables. To avoid multicollinearity issues in the model selection process, we only included a set of predictors where no correlations with $r < -0.6$ or $r > 0.6$ were present. This approach ensured that predictors in the models were independent, reducing multicollinearity issues. We used the function dredge() from the *MuMIn* package (version 1.47.5) with default settings for automated model selection based on the Akaike information criterion corrected for small sample sizes. Moreover, we checked the spatial autocorrelation among the residuals of the fitted model using the *ape* package (version 5.7.1).

Overall, the best-fit model was selected with the continuous predictor variables of elevation, northness of aspect, soil pH, number of trees, tree species diversity, MH, mean annual precipitation, MAT, and distance from the nearest settlement. Variables, such as the number of trees and settlement distance, were log-transformed for both simple and multiple linear regressions, because they were highly right-skewed when visibly assessing their distribution.

Results

Plot-level characteristics

Based on our fieldwork observations, we gathered data from forests of 3 disturbance categories: undisturbed (46 plots), moderately disturbed (17 plots), and highly disturbed (6 plots). Based on 1677 trees of 53 species, among which *Alnus nepalensis* D. don., *Pinus wallichiana* A.B. Jacks., *Daphniphyllum himalense* (Benth.) Müll. Arg., *Rhododendron* spp, and *Abies pindrow* Royle were most dominant, we categorized the forests as consisting of 3 main plant functional types: EBT (29 plots), DBT (16 plots), and ENT (24 plots). We observed plot-level FSC in terms of the value of D_b, which ranged from a minimum of 1.8 to a maximum of 2.6 (Appendix S1, *Supplemental material,* https://doi.org/10.1659/mrd.2024.00009. S1). D_b can only range from 1 (corresponding to a single tree

TABLE 1 Linear regression coefficients for each explanatory variable of D_b.

Explanatory variable	Coefficient (β)	SE	P	R^2
Elevation	−7.83	2.86	0.780	0.01
Shannon diversity index	0.06	0.03	0.042*	0.06
Number of trees (log)	0.35	0.05	<0.001*	0.42
Northness	0.07	0.02	0.003*	0.12
Precipitation	0	0	0.269	0.02
MH (polynomial)	—	0.11	<0.001*	0.45
Settlement distance (log)	0.13	0.04	0.001*	0.14
Soil pH	−0.10	0.04	0.027*	0.07
MAT	0	0	0.848	0.01

* $P < 0.05$.

without branches) to a theoretical maximum of 3 (a solid cube filled entirely with plant material).

Drivers of D_b regression analysis

We discovered that several factors influence FSC (D_b; Table 1). The number of trees, settlement distance, northness of aspect, and Shannon index value for tree species diversity showed a significant positive relationship with D_b. The MH and soil pH values had a significant negative effect on D_b. We found that precipitation, elevation, and MAT did not have a significant relationship with D_b (Figure 2).

We also found that the overall level of forest disturbance had a significant impact on FSC ($\chi^2 = 10.91$, $P < 0.01$). Undisturbed plots had a significantly higher D_b than both moderately disturbed ($P < 0.05$) and highly disturbed ($P < 0.05$) plots when comparing each level of disturbance (Figure 3A). Correspondingly, we observed a noteworthy effect of plant functional type on D_b ($\chi^2 = 7.92$, $P < 0.05$). EBT showed higher D_b than both ENT ($P < 0.05$) and DBT ($P < 0.05$; Figure 3B).

Correlation among predictor variables

We observed a high correlation between some explanatory variables, such as elevation, MAT, and soil pH, as well as between precipitation and soil pH (Figure 4). Furthermore, we realized that the distance of the nearest settlement from a plot showed significant correlation with tree numbers within the plot. Therefore, the final model was fitted with tree numbers, MH, species diversity, northness of aspect, and soil pH variables.

Fitted model for D_b

In our analysis, all measured factors were also employed as predictor variables to explain FSC. It revealed that variables, namely, the number of trees, species diversity, and MH, significantly influenced FSC (Table 1). Although northness of aspect and soil pH were found to collectively explain the variation in FSC, we discovered that the settlement distance variable did not fit this model well.

The fitted model demonstrated a significant association with D_b, as shown by an adjusted R^2 value of 0.60 ($P < 0.001$,

residual SE = 0.08). Furthermore, we conducted a Moran I test on residuals of the model, revealing no significant evidence of spatial autocorrelation ($P < 0.05$).

The following explanatory variables were used to define FSC, D_b, modeled using Equation 1:

$$D_b = 2.62 + 0.2\log_{10}nTrees - 0.13MH - 0.45MH^2 + 0.01MH^3$$
$$+ 0.04sDiversity + 0.05northness - 0.09soilpH \qquad (1)$$

where D_b represents FSC; $\log_{10}nTrees$ corresponds to the logarithm (base 10) of the number of trees present in the plot; $sDiversity$ represents the Shannon index, which quantifies the diversity of tree species; $northness$ represents the aspect of the forest location; and $soilpH$ denotes the acidity or alkalinity value of the forest soil.

Equation 1 showed that D_b representing FSC is positively influenced by the number of trees, tree species diversity, and northness of aspect. In contrast, it is negatively influenced by MH and soil pH. The fitted equation also showed that MH had a nonlinear effect on D_b, with a cubic term that captures the curvature of the relationship. The equation also showed that the number of trees has a logarithmic effect on D_b, which means that the marginal increase in FSC decreases as the number of trees increases. Climatic and elevational variables had no discernible impact on the model.

Discussion

Our approach to FSC, namely, D_b from laser scanning, has previously been applied to different forest types and proved useful across scales and biomes from tree level (eg Seidel 2018; Saarinen et al 2020; Arseniou et al 2021; Dorji et al 2021; Heidenreich and Seidel 2022; Mathes et al 2023) to stand level (Seidel et al 2020; Camarretta et al 2021; Neudam et al 2022). Within a biome, there is evidence for increased D_b with an increasing degree of maturity in the forest structure, with the highest values in old-growth forests. This was shown in earlier studies in both temperate forests (eg Stiers et al 2020) and tropical forests (Camarretta et al 2021). According to our research, the distance of a forest from the nearest settlement, as a quantitative measure of disturbance likelihood, is also a significant factor for FSC

FIGURE 2 Scatterplots showing the individual relationships between continuous explanatory variables and FSC. Linear regression analysis was employed to model the relationship between FSC, represented by D_b, and (A) elevation (in meters), (B) Shannon index value for tree species diversity, (C) number of trees (log), (D) northness of aspect, (E) precipitation (in millimeters per year), (G) distance of the nearest settlement from the plot, (H) soil pH, and (I) MAT (in degrees Celsius). (F) Polynomial regression (3-degree) model fitted for D_b from MH (in meters). The shaded portion in each plot represents the predictions, along with their 95% confidence intervals, derived from the linear model.
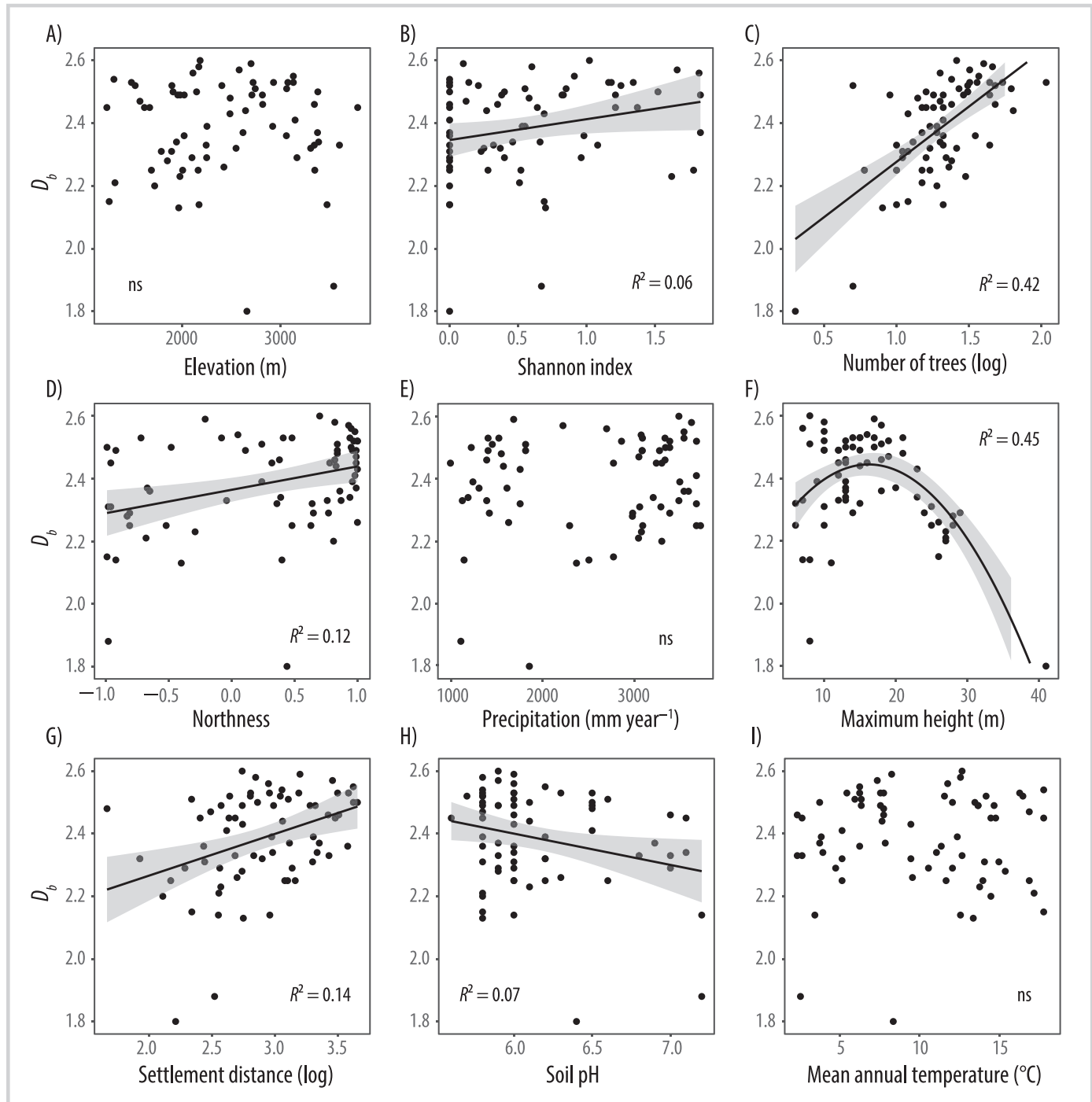

(Figure 2G) of Himalayan forests (Måren et al 2015; Verma et al 2021). When a forest is located near a settlement, it often experiences higher levels of human activity, such as livestock grazing, fires, logging, or collection of forest products (Tietema et al 1991; Shackleton et al 1994). This can lead to structural changes and, if the forest was previously in pristine condition, almost always to a reduction in FSC (Seidel and Ammer 2023). In contrast, in some specific cases,

less frequent forest fires have altered monospecific stands (eg *Pinus* spp and *Rhododendron* spp) toward species-rich forests, which may alter FSC (Bargali et al 2022). However, the case of the Himalayan forests studied here supports the argument that disturbance has a negative effect on FSC (Figure 3A; settlement distance in Table 1).

Our results from the Annapurna region further revealed a significantly higher complexity of forests dominated by

FIGURE 3 Box plots illustrating the D_b value for (A) 3 levels of forest disturbance (UD, undisturbed; MD, moderately disturbed; and HD, highly disturbed), and (B) 3 forest types (EBT, ENT, and DBT). Differences between pairs of groups were tested for significance with the Kruskal–Wallis test, followed by the Dunn test for pairwise comparisons; *$P < 0.05$, **$P < 0.01$.
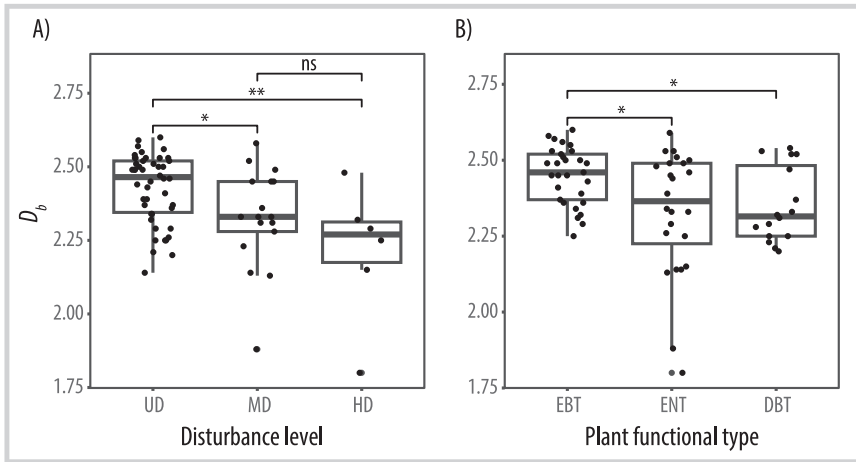
EBT compared with ENT and DBT species (Figure 3B). Despite the known positive effect of leaves on FSC of individual trees (Arseniou et al 2021) and entire forests (Neudam et al 2022), we argue that the observed differences in our study are linked to overall differences in tree architecture of the different dominating species. Leaf effects were reported to be on the order of 0.04 units of D_b for beech forests (Neudam et al 2022). The differences among forest types observed in our study are larger and cannot be explained by the potential effects of leaf shedding that we observed in some plots. However, the DBT

species mainly occurred in lower-elevation belts, where forests were managed as monoculture (eg *Alnus* spp and *Pinus* spp) with the presence of high levels of human activity. We argue that this management and human disturbance are likely the major drivers of the lower FSC in these forests. The forests dominated by EBT species (eg *Rhododendron* spp and *Quercus* spp) were least disturbed and of greater species diversity (mean Shannon index: EBT = 0.89, DBT = 0.27, ENT = 0.42; Appendix S1, *Supplemental material,* https://doi.org/10.1659/mrd.2024.00009.S1), with plenty of undergrowth seedlings and saplings.

FIGURE 4 Correlogram showing Pearson's correlation coefficient of each pair of explanatory variables and FSC represented by plot-level D_b. *Elevation* denotes the topographical elevation (in meters above sea level), *northness* values range from +1 (exactly north) to −1 (exactly south), *precipitation* represents accumulated annual precipitation (in millimeters per year), and *sDistance* represents the distance between each plot and the nearest settlement.
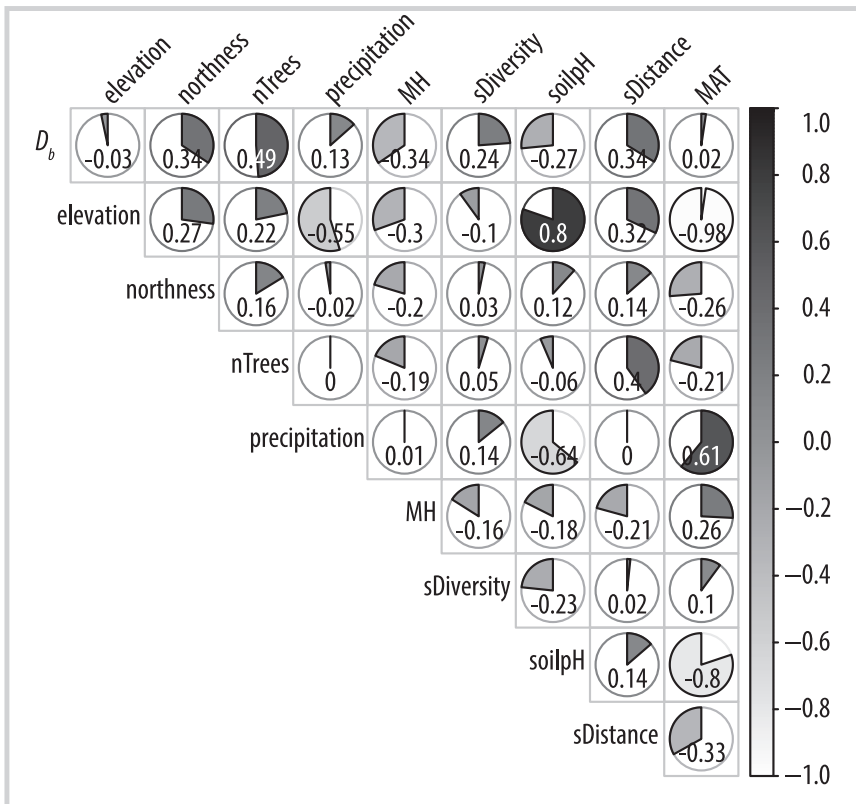
The observed positive relationship between tree species diversity and FSC (Figure 2B) confirms earlier findings (Ehbrecht et al 2017; Juchheim et al 2019). A forest with a greater variety of tree species supports a more diverse range of tree shapes, sizes, morphologies, and occupied niches (Liu et al 2018). This, in turn, increases the likelihood of the formation of a denser and more complex forest with multiple layers, as opposed to a forest dominated by a single species (Ashton and Ducey 1997).

The positive effect of the number of trees on the plot-level FSC observed here (Figure 2C) confirms earlier findings (eg Spies and Franklin 1991). Lower numbers of trees often indicate highly disturbed sites or forests that are characterized by only a few large dominant trees. Such forests hardly ever possess the vertical layering required for high FSC (cf Seidel and Ammer 2023). Upon examining the relationships between predictor variables, such as number of trees and settlement distance from the forest, we found that only the number of trees significantly affected FSC (Equation 1). This is because settlement distance is a measure of disturbance within the forest, and forests near settlements tend to experience greater anthropogenic pressure, resulting in a lower number of trees (Verma et al 2021).

The existence of taller trees in a forest, here approximated by MH, was expected to be positively related to FSC, according to earlier findings (Seidel, Ehbrecht, Annighöfer, et al 2019). Tall trees tend to possess a greater individual tree structural complexity than small trees, which should positively affect stand-level FSC (Seidel, Ehbrecht, Dorji, et al 2019). However, our study revealed a nonlinear correlation between the MH of the stand and its FSC (Figure 2F). FSC increased with MH approaching 15 m, stagnated until 20 m, and then quickly dropped with MH increasing further. We argue that this pattern can be explained by large dominant overstory trees hampering understory growth. In mountain regions in particular, this affects FSC in the understory negatively and creates forests with little structural complexity because of limited light availability and allelopathic effects (Royo and Carson 2006; Dormann et al 2020; Schickhoff et al 2023).

Our study revealed a significant inverse relationship between Himalayan FSC and soil pH levels (Figure 2H). Specifically, as soil pH increases, FSC decreases in this region. Furthermore, soil alkalinity tended to rise with an increase in elevational range (Figure 4) but only under specific conditions in which the parent material, weathering processes, vegetation, and climate remain similar (Zhang et al 2019). In our study area, characterized by geologically distinct substrates such as gneiss and migmatite, where fluvial calcareous parent soils are more frequent with elevation, an increase in soil alkalinity is logical (NARC nd). The lower air temperature and higher soil alkalinity found at higher elevations result in reduced organic carbon content and reduced availability of essential nutrients (eg nitrogen and potassium) in the soil, which in turn lead to a reduction in FSC with increasing elevation (Måren et al 2015; Müller et al 2017). However, our findings do not demonstrate any impact of elevation and temperature on FSC. We argue that this is likely because the forests analyzed in this study ranged from 1200 to 3800 m in elevation, with 85% of the forests below 3200 m in elevation (Appendix S1, *Supplemental material,* https://doi.org/10.1659/mrd.2024.00009.S1). The tree line

elevation in the Himalayan region typically ranges from 3200 to 4900 m and can extend even higher in some areas (Pratap Singh et al 2019). Therefore, the forest plots we examined are all situated within an elevational range that still supports growth. Moreover, the average surface air temperature in the Himalayan region has doubled since 1951, compared with the preceding period, indicating a significant warming trend (Sabin et al 2020). In our study region, MAT ranges from 2.35 to 17.75°C (Appendix S1, *Supplemental material,* https://doi.org/10.1659/mrd.2024.00009.S1), which can be sufficient for forest growth. Several studies suggest that the warming trend in the Himalayan region is reducing temperature limitations on forest growth and is associated with an increase in plant species diversity (Telwala et al 2013; Shi et al 2020; Gaire et al 2023). Given that the temperature in this region falls within a range conducive to forest growth, it is possible that both temperature and elevation variables may not exert a significant influence on FSC (Figure 2A, I; Pandey et al 2016).

However, our findings indicate that forests on the northern slope of the Annapurna range are more structurally complex than those on the southern slope (Figure 2D). This is likely because of the higher moisture levels in the soil on the northern slope than those on the southern slope, which receives more direct sunlight, resulting in drier soil. Although forests in warmer temperatures tend to grow well with adequate moisture, the southern slope of the Himalayas has steep terrain that drains precipitation and allows direct sunlight to dry out the soil, leading to a lack of moisture (Srivastava et al 2010). As a result, the northern slope is able to support a more complex vegetation structure, as observed in our data. Overall, it seems that in mountain forests, aspect is more relevant than actual precipitation amounts (Carpenter and Zomer 1996). Accordingly, although previous studies identified precipitation as a major predictor for FSC on the global scale (Ehbrecht et al 2021), we could not support such a finding based on our data (Figure 2E). However, we argue that this was simply because the forests studied here all received sufficient precipitation, with a minimum mean annual precipitation close to 1000 mm (Appendix S1, *Supplemental material,* https://doi.org/10.1659/mrd.2024.00009.S1). Therefore, it appears that precipitation was not a limiting factor at any of our plots. At the same time, the local topographical conditions, such as aspect, are crucial factors affecting the actual amount of water available to plants and hence FSC. Aspect has been reported as a factor that determines forest communities in mountain forests, with positive and negative effects possible (Fontaine et al 2007; Heiri et al 2009).

Given the importance of FSC, particularly for maximizing the adaptive capacity of the ecosystem (Seidel and Ammer 2023), it is strongly recommended that the findings presented here be incorporated into the preparation and monitoring of management and protection plans for forests in the area. This means management should target the creation or, where already present, the conservation of complex forest structures. These can be found in forests comprising large numbers of trees of different species. In the present study, such forests were of intermediate height (MH of ~20 m) and mostly found at greater distances from settlements on sites with low pH that faced north. It appears that complex forests can potentially be found anywhere in the investigated range

without clear effects of precipitation, temperature, or elevation in general.

Conclusion

Our study on forests of the Annapurna Himalayan region found that the number of trees, MH, species diversity, northness aspect, soil pH, and forest disturbance are critical factors that influence FSC. Contrary to previous findings, climatic factors like precipitation and temperature did not affect FSC in the area, likely because of they exceeded the necessary minima required for forest growth. This underscores the uniqueness of the Himalayan forest environment and highlights the need for region-specific conservation and management strategies. In light of our findings, we conclude that efforts to preserve or reestablish FSC in forests of the Himalayas should adopt a mixed species, multistoried forest management approach. By prioritizing these key factors, we can better safeguard the ecological integrity and biodiversity of this remarkable mountain ecosystem. Ultimately, this research can serve as a foundation for sustainable forest management practices by using D_b as a tool to monitor FSC over time or for benchmarking certain levels of FSC.

REFERENCES

Ali A, Lin S-L, He J-K, Kong F-M, Yu J-H, Jiang H-S. 2019. Climate and soils determine aboveground biomass indirectly via species diversity and stand structural complexity in tropical forests. *Forest Ecology and Management* 432:823–831. https://doi.org/10.1016/j.foreco.2018.10.024.

Arseniou G, MacFarlane DW, Seidel D. 2021. Measuring the contribution of leaves to the structural complexity of urban tree crowns with terrestrial laser scanning. *Remote Sensing* 13(14):2773. https://doi.org/10.3390/rs13142773.

Asbeck T, Frey J. 2021. Weak relationships of continuous forest management intensity and remotely sensed stand structural complexity in temperate mountain forests. *European Journal of Forest Research* 140(3):721–731. https://doi.org/10.1007/s10342-021-01361-4.

Ashton PMS, Ducey M. 1997. The development of mixed species plantations as successional analogues to natural forests. *In:* Northeastern Forest Nursery Association, editor. *National Proceedings, Forest and Conservation Nursery Associations.* Portland, OR: US Department of Agriculture, Forest Service, Pacific Northwest Research Station, pp 113–126.

Atkins JW, Bohrer G, Fahey RT, Hardiman BS, Morin TH, Stovall AEL, Zimmerman N, Gough CM. 2018. Quantifying vegetation and canopy structural complexity from terrestrial LiDAR data using the forestr r package. *Methods in Ecology and Evolution* 9(10):2057–2066. https://doi.org/10.1111/2041-210X.13061.

Barbeito I, Dassot M, Bayer D, Collet C, Drössler L, Löf M, del Rio M, Ruiz-Peinado R, Forrester DI, Bravo-Oviedo A, et al. 2017. Terrestrial laser scanning reveals differences in crown structure of *Fagus sylvatica* in mixed vs. pure European forests. *Forest Ecology and Management* 405:381–390. https://doi.org/10.1016/j.foreco.2017.09.043.

Bargali H, Calderon LPP, Sundriyal R, Bhatt D. 2022. Impact of forest fire frequency on floristic diversity in the forests of Uttarakhand, western Himalaya. *Trees, Forests and People* 9:100300. https://doi.org/10.1016/j.tfp.2022.100300.

Braunisch V, Roder S, Coppes J, Froidevaux JSP, Arlettaz R, Bollmann K. 2019. Structural complexity in managed and strictly protected mountain forests: Effects on the habitat suitability for indicator bird species. *Forest Ecology and Management* 448:139–149. https://doi.org/10.1016/j.foreco.2019.06.007.

Camarretta N, Ehbrecht M, Seidel D, Wenzel A, Zuhdi M, Merk MS, Schlund M, Erasmi S, Knohl A. 2021. Using airborne laser scanning to characterize land-use systems in a tropical landscape based on vegetation structural metrics. *Remote Sensing* 13(23):4794. https://doi.org/10.3390/rs13234794.

Carpenter C, Zomer R. 1996. Forest ecology of the Makalu-Barun National Park and Conservation Area, Nepal. *Mountain Research and Development* 16(2):135–148. https://doi.org/10.2307/3674007.

Chaudhary RP, Uprety Y, Rimal SK. 2016. Chapter 12.2. Deforestation in Nepal: Causes, consequences, and responses. *In:* Shroder JF, Sivanpillai R, editors. *Biological and Environmental Hazards, Risks, and Disasters.* Boston, MA: Academic, pp 335–372. https://doi.org/10.1016/B978-0-12-394847-2.00020-6.

Dasgupta P, Shakya B. 2023. Ecosystem services as systemic enablers for transformation in the Hindu Kush Himalaya: An analytical synthesis. *Regional Environmental Change* 23(1):39. https://doi.org/10.1007/s10113-022-02022-x.

Dorji Y, Schuldt B, Neudam L, Dorji R, Middleby K, Isasa E, Körber K, Ammer C, Annighöfer P, Seidel D. 2021. Three-dimensional quantification of tree architecture from mobile laser scanning and geometry analysis. *Trees* 35(4):1385–1398. https://doi.org/10.1007/s00468-021-02124-9.

Dormann CF, Bagnara M, Boch S, Hinderling J, Janeiro-Otero A, Schäfer D, Schall P, Hartig F. 2020. Plant species richness increases with light availability, but not variability, in temperate forests understorey. *BMC Ecology* 20(1):43. https://doi.org/10.1186/s12898-020-00311-9.

Dubayah R, Armston J, Healey SP, Bruening JM, Patterson PL, Kellner JR, Duncanson L, Saarela S, Ståhl G, Yang Z, et al. 2022. GEDI launches a new era of biomass inference from space. *Environmental Research Letters* 17(9):095001. https://doi.org/10.1088/1748-9326/ac8694.

Ehbrecht M, Schall P, Ammer C, Seidel D. 2017. Quantifying stand structural complexity and its relationship with forest management, tree species diversity and microclimate. *Agricultural and Forest Meteorology* 242:1–9. https://doi.org/10.1016/j.agrformet.2017.04.012.

Ehbrecht M, Seidel D, Annighöfer P, Kreft H, Köhler M, Zemp DC, Puettmann K, Nilus R, Babweteera F, Willim K, et al. 2021. Global patterns and climatic controls of forest structural complexity. *Nature Communications* 12(1):519. https://doi.org/10.1038/s41467-020-20767-z.

Fontaine M, Aerts R, Özkan K, Mert A, Gülsoy S, Süel H, Waelkens M, Muys B. 2007. Elevation and exposition rather than soil types determine communities and site suitability in Mediterranean mountain forests of southern Anatolia, Turkey. *Forest Ecology and Management* 247(1):18–25. https://doi.org/10.1016/j.foreco.2007.04.021.

Gaire NP, Zaw Z, Bräuning A, Grießinger J, Sharma B, Rana P, Bhandari S, Basnet S, Fan Z-X. 2023. The impact of warming climate on Himalayan silver fir growth along an elevation gradient in the Mt. Everest region. *Agricultural and Forest Meteorology* 339:109575. https://doi.org/10.1016/j.agrformet.2023.109575.

Heidenreich MG, Seidel D. 2022. Assessing forest vitality and forest structure using 3D data: A case study from the Hainich National Park, Germany. *Frontiers in Forests and Global Change* 5. https://doi.org/10.3389/ffgc.2022.929106.

Heiri C, Wolf A, Rohrer L, Bugmann H. 2009. Forty years of natural dynamics in Swiss beech forests: Structure, composition, and the influence of former management. *Ecological Applications* 19(7):1920–1934. https://doi.org/10.1890/08-0516.1.

Juchheim J, Ehbrecht M, Schall P, Ammer C, Seidel D. 2019. Effect of tree species mixing on stand structural complexity. *Forestry: An International Journal of Forest Research* 93(1):75–83. https://doi.org/10.1093/forestry/cpz046.

Karger DN, Conrad O, Böhner J, Kreft H, Soria-Auza RW, Zimmermann NE, Linder HP, Kessler M. 2017. Climatologies at high resolution for the Earth's land surface areas. *Scientific Data* 4:170122. https://doi.org/10.1038/sdata.2017.122.

Kassambara A. 2023. *ggpubr: ''ggplot2'' Based Publication Ready Plots. R Package Version 0.6.0.* Vienna, Austria: CRAN [Comprehensive R Archive Network]. https://CRAN.R-project.org/package=ggpubr; accessed on 3 January 2024.

Kattel GR. 2022. Climate warming in the Himalayas threatens biodiversity, ecosystem functioning and ecosystem services in the 21st century: Is there a better solution? *Biodiversity and Conservation* 31(8):2017–2044. https://doi.org/10.1007/s10531-022-02417-6.

Kleinn C, Traub B, Hoffmann C. 2002. A note on the slope correction and the estimation of the length of line features. *Canadian Journal of Forest Research* 32(4):751–756. https://doi.org/10.1139/x02-004.

Liu CLC, Kuchma O, Krutovsky KV. 2018. Mixed-species versus monocultures in plantation forestry: Development, benefits, ecosystem services and perspectives for the future. *Global Ecology and Conservation* 15:e00419. https://doi.org/10.1016/j.gecco.2018.e00419.

Ma Q, Su Y, Hu T, Jiang L, Mi X, Lin L, Cao M, Wang X, Lin F, Wang B, et al. 2022. The coordinated impact of forest internal structural complexity and tree species diversity on forest productivity across forest biomes. *Fundamental Research* 4(5):1185–1195. https://doi.org/10.1016/j.fmre.2022.10.005.

Mandelbrot BB. 1982. *The Fractal Geometry of Nature* (revised edition). San Francisco, CA: Freeman.

Måren IE, Karki S, Prajapati C, Yadav RK, Shrestha BB. 2015. Facing north or south: Does slope aspect impact forest stand characteristics and soil properties in a semiarid trans-Himalayan valley? *Journal of Arid Environments* 121:112–123. https://doi.org/10.1016/j.jaridenv.2015.06.004.

Mathes T, Seidel D, Häberle K-H, Pretzsch H, Annighöfer P. 2023. What are we missing? Occlusion in laser scanning point clouds and its impact on the detection of single-tree morphologies and stand structural variables. *Remote Sensing* 15(2):450. https://doi.org/10.3390/rs15020450.

Miehe G, Pendry CA, Chaudhary RP. 2015. *Nepal: An Introduction to the Natural History, Ecology and Human Environment in the Himalayas.* Edinburgh, United Kingdom: Royal Botanic Garden.

Müller M, Oelmann Y, Schickhoff U, Böhner J, Scholten T. 2017. Himalayan treeline soil and foliar C:N:P stoichiometry indicate nutrient shortage with

elevation. *Geoderma* 291:21–32. https://doi.org/10.1016/j.geoderma.2016. 12.015.

NARC [National Soil Science Research Centre]. nd. *Soil Map.* Kathmandu, Nepal: NARC. https://soil.narc.gov.np/soil/soilmap/; accessed on 21 September 2023.

NASA JPL [National Aeronautics and Space Administration Jet Propulsion Laboratory]. 2013. *SRTMGL30 v021. NASA Shuttle Radar Topography Mission Global 30 arc second* [dataset]. Sioux Falls, SD: NASA EOSDIS [Earth Observing System Data and Information System] Land Processes Distributed Active Archive Center. https://doi.org/10.5067/MEASURES/SRTM/SRTMGL30.002; accessed on 18 April 2022.

Neudam L, Annighöfer P, Seidel D. 2022. Exploring the potential of mobile laser scanning to quantify forest structural complexity. *Frontiers in Remote Sensing* 3:861337. https://doi.org/10.3389/frsen.2022.861337.

Pandey KP. 2016. Structure, composition and diversity of forest along the altitudinal gradient in the Himalayas, Nepal. *Applied Ecology and Environmental Research* 14(2):235–251. https://doi.org/10.15666/aeer/1402_235251.

Poggio L, de Sousa LM, Batjes NH, Heuvelink GBM, Kempen B, Ribeiro E, Rossiter D. 2021. SoilGrids 2.0: Producing soil information for the globe with quantified spatial uncertainty. *SOIL* 7(1):217–240. https://doi.org/10.5194/soil-7-217-2021.

Potapov P, Li X, Hernandez-Serna A, Tyukavina A, Hansen MC, Kommareddy A, Pickens A, Turubanova S, Tang H, Silva CE, et al. 2021. Mapping global forest canopy height through integration of GEDI and Landsat data. *Remote Sensing of Environment* 253:112165. https://doi.org/10.1016/j.rse.2020.112165.

Pratap Singh S, Sharma S, Dhyani P. 2019. Himalayan arc and treeline: Distribution, climate change responses and ecosystem properties. *Biodiversity and Conservation* 28:1997–2016. https://doi.org/10.1007/s10531-019-01777-w.

Qi Y, Coops NC, Daniels LD, Butson CR. 2022. Comparing tree attributes derived from quantitative structure models based on drone and mobile laser scanning point clouds across varying canopy cover conditions. *ISPRS Journal of Photogrammetry and Remote Sensing* 192:49–65. https://doi.org/10.1016/j.isprsjprs.2022.07.021.

R Core Team. 2023. *R: A Language and Environment for Statistical Computing.* Vienna, Austria: R Core Team. https://www.R-project.org/; accessed on 30 August 2023.

Rahbek C, Borregaard MK, Colwell RK, Dalsgaard B, Holt BG, Morueta-Holme N, Nogues-Bravo D, Whittaker RJ, Fjeldsä J. 2019. Humboldt's enigma: What causes global patterns of mountain biodiversity? *Science* 365(6458):1108–1113. https://doi.org/10.1126/science.aax0149.

Royo AA, Carson WP. 2006. On the formation of dense understory layers in forests worldwide: consequences and implications for forest dynamics, biodiversity, and succession. *Canadian Journal of Forest Research* 36(6):1345–1362. https://doi.org/10.1139/x06-025.

Saarinen N, Kankare V, Yrttimaa T, Viljanen N, Honkavaara E, Holopainen M, Hyyppä J, Huuskonen S, Hynynen J, Vastaranta M. 2020. Assessing the effects of thinning on stem growth allocation of individual Scots pine trees. *Forest Ecology and Management* 474:118344. https://doi.org/10.1016/j.foreco.2020.118344.

Sabin TP, Krishnan R, Vellore R, Priya P, Borgaonkar HP, Singh BB, Sagar A. 2020. Climate change over the Himalayas. *In:* Krishnan R, Sanjay J, Gnanaseelan C, Mujumdar M, Kulkarni A, Chakraborty S, editors. *Assessment of Climate Change over the Indian Region: A Report of the Ministry of Earth Sciences (MoES), Government of India.* Singapore: Springer, pp 207–222. https://doi.org/10.1007/978-981-15-4327-2_11.

Schickhoff U, Bobrowski M, Böhner J, Bürzle B, Chaudhary RP, Müller M, Scholten T, Schwab N, Weidinger J. 2023. The treeline ecotone in Rolwaling Himal, Nepal: Pattern–process relationships and treeline shift potential. *In:* Singh SP, Reshi ZA, Joshi R, editors. *Ecology of Himalayan Treeline Ecotone.* Singapore: Springer, pp 95–145. https://doi.org/10.1007/978-981-19-4476-5_5.

Schmeller DS, Urbach D, Bates K, Catalan J, Cogălniceanu D, Fisher MC, Friesen J, Füreder L, Gaube V, Haver M, et al. 2022. Scientists' warning of threats to mountains. *Science of the Total Environment* 853:158611. https://doi.org/10.1016/j.scitotenv.2022.158611.

Seidel D. 2018. A holistic approach to determine tree structural complexity based on laser scanning data and fractal analysis. *Ecology and Evolution* 8(1):128–134. https://doi.org/10.1002/ece3.3661.

Seidel D, Ammer C. 2023. Towards a causal understanding of the relationship between structural complexity, productivity, and adaptability of forests based on principles of thermodynamics. *Forest Ecology and Management* 544:121238. https://doi.org/10.1016/j.foreco.2023.121238.

Seidel D, Annighöfer P, Ehbrecht M, Magdon P, Wöllauer S, Ammer C. 2020. Deriving stand structural complexity from airborne laser scanning data: What does it tell us about a forest? *Remote Sensing* 12(11):1854. https://doi.org/10.3390/rs12111854.

Seidel D, Ehbrecht M, Annighöfer P, Ammer C. 2019. From tree to stand-level structural complexity: Which properties make a forest stand complex?

Agricultural and Forest Meteorology 278:107699. https://doi.org/10.1016/j.agrformet.2019.107699.

Seidel D, Ehbrecht M, Dorji Y, Jambay J, Ammer C, Annighöfer P. 2019. Identifying architectural characteristics that determine tree structural complexity. *Trees* 33(3):911–919. https://doi.org/10.1007/s00468-019-01827-4.

Seidel D, Ehbrecht M, Puettmann K. 2016. Assessing different components of three-dimensional forest structure with single-scan terrestrial laser scanning: A case study. *Forest Ecology and Management* 381:196–208. https://doi.org/10.1016/j.foreco.2016.09.036.

Shackleton CM, Griffin NJ, Banks DI, Mavrandonis JM, Shackleton SE. 1994. Community structure and species composition along a disturbance gradient in a communally managed South African savanna. *Vegetatio* 115(2):157–167. https://doi.org/10.1007/BF00044870.

Shahgedanova M, Adler C, Gebrekirstos A, Grau HR, Huggel C, Marchant R, Pepin N, Vanacker V, Viviroli D, Vuille M. 2021. Mountain observatories: Status and prospects for enhancing and connecting a global community. *Mountain Research and Development* 41(2):A1. https://doi.org/10.1659/MRD-JOURNAL-D-20-00054.1.

Shi C, Schneider L, Hu Y, Shen M, Sun C, Xia J, Forbes BC, Shi P, Zhang Y, Ciais P. 2020. Warming-induced unprecedented high-elevation forest growth over the monsoonal Tibetan Plateau. *Environmental Research Letters* 15(5):054011. https://doi.org/10.1088/1748-9326/ab7b9b.

Spies TA, Franklin JF. 1991. The structure of natural young, mature, and old-growth Douglas-fir forests in Oregon and Washington. *In*: Ruggiero LF, Aubry KB, Carey AB, Huff MH, editors. *Wildlife and Vegetation of Unmanaged Douglas-Fir Forests.* General Technical Report PNW-285. Portland, OR: US Department of Agriculture, Forest Service Pacific Northwest Research Station, pp 91–109. https://andrewsforest.oregonstate.edu/publications/1244; accessed on 30 June 2023.

Srivastava V, Srivastava HB, Lakhera RC. 2010. Fuzzy gamma based geomatic modelling for landslide hazard susceptibility in a part of Tons river valley, northwest Himalaya, India. *Geomatics, Natural Hazards and Risk* 1(3):225–242. https://doi.org/10.1080/19475705.2010.490103.

Stiers M, Annighöfer P, Seidel D, Willim K, Neudam L, Ammer C. 2020. Quantifying the target state of forest stands managed with the continuous cover approach: Revisiting Möller's "Dauerwald" concept after 100 years. *Trees, Forests and People* 1:100004. https://doi.org/10.1016/j.tfp.2020.100004.

Stiers M, Willim K, Seidel D, Ehbrecht M, Kabal M, Ammer C, Annighöfer P. 2018. A quantitative comparison of the structural complexity of managed, lately unmanaged and primary European beech (*Fagus sylvatica* L.). *Forest Ecology and Management* 430:357–365. https://doi.org/10.1016/j.foreco.2018.08.039.

Telwala Y, Brook BW, Manish K, Pandit MK. 2013. Climate-induced elevational range shifts and increase in plant species richness in a Himalayan biodiversity epicentre. *PLoS ONE* 8(2):e57103. https://doi.org/10.1371/journalpone.0057103.

Tietema T, Tolsma DJ, Veenendaal EM, Schroten J. 1991. Plant responses to human activities in the tropical savanna ecosystem of Botswana. *In:* Rozema J, Verkleij JAC, editors. *Ecological Responses to Environmental Stresses.* Dordrecht, the Netherlands: Springer, pp 262–277. https://doi.org/10.1007/978-94-009-0599-3_23.

Verma A, Schmidt-Vogt D, De Alban JDT, Lim CL, Webb EL. 2021. Drivers and mechanisms of forest change in the Himalayas. *Global Environmental Change* 68:102–244. https://doi.org/10.1016/j.gloenvcha.2021.102244.

Walter JA, Stovall AEL, Atkins JW. 2021. Vegetation structural complexity and biodiversity in the Great Smoky Mountains. *Ecosphere* 12(3):e03390. https://doi.org/10.1002/ecs2.3390.

Wang Y, Wu N, Kunze C, Long R, Perlik M. 2019. Drivers of change to mountain sustainability in the Hindu Kush Himalaya. *In:* Wester P, Mishra A, Mukherji A, Shrestha AB, editors. *The Hindu Kush Himalaya Assessment: Mountains, Climate Change, Sustainability and People.* Cham, Switzerland: Springer, pp 17–56. https://doi.org/10.1007/978-3-319-92288-1_2.

Willim K, Ammer C, Seidel D, Annighöfer P, Schmucker J, Schall P, Ehbrecht M. 2022. Short-term dynamics of structural complexity in differently managed and unmanaged European beech forests. *Trees, Forests and People* 8:100231. https://doi.org/10.1016/j.tfp.2022.100231.

Wiltshire AJ. 2014. Climate change implications for the glaciers of the Hindu Kush, Karakoram and Himalayan region. *The Cryosphere* 8(3):941–958. https://doi.org/10.5194/tc-8-941-2014.

Zhang Y-Y, Wu W, Liu H. 2019. Factors affecting variations of soil pH in different horizons in hilly regions. *PLoS ONE* 14(6):e0218563. https://doi.org/10.1371/journalpone.0218563.

Supplemental material

APPENDIX S1 Overview of the key characteristics of the study plots.